

ARTICLE OPEN



Positron emission tomography imaging of serotonin degeneration and beta-amyloid deposition in late-life depression evaluated with multi-modal partial least squares

Gwenn S. Smith^{1,2,7}, Clifford I. Workman^{1,7}, Hillary Protas³, Yi Su³, Alena Savonenko⁴, Hiroto Kuwabara², Neda F. Gould¹, Michael Kraut⁵, Jin Hui Joo¹, Ayon Nandi², Dimitri Avramopoulos⁶, Eric M. Reiman³ and Kewei Chen³

© The Author(s) 2021

Depression in late-life is associated with increased risk of cognitive decline and development of all-cause dementia. The neurobiology of late-life depression (LLD) may involve both neurochemical and neurodegenerative mechanisms that are common to depression and dementia. Transgenic amyloid mouse models show evidence of early degeneration of monoamine systems. Informed by these preclinical data, the hypotheses were tested that a spatial covariance pattern of higher beta-amyloid (A β) and lower serotonin transporter availability (5-HTT) in frontal, temporal, and parietal cortical regions would distinguish LLD patients from healthy controls and the expression of this pattern would be associated with greater depressive symptoms. Twenty unmedicated LLD patients who met DSM-V criteria for major depression and 20 healthy controls underwent PET imaging with radiotracers for A β ([¹¹C]-PiB) and 5-HTT ([¹¹C]-DASB). A voxel-based multi-modal partial least squares (mmPLS) algorithm was applied to the parametric PET images to determine the spatial covariance pattern between the two radiotracers. A spatial covariance pattern was identified, including higher A β in temporal, parietal and occipital cortices associated with lower 5-HTT in putamen, thalamus, amygdala, hippocampus and raphe nuclei (dorsal, medial and pontine), which distinguished LLD patients from controls. Greater expression of this pattern, reflected in summary 5-HTT/A β mmPLS subject scores, was associated with higher levels of depressive symptoms. The mmPLS method is a powerful approach to evaluate the synaptic changes associated with AD pathology. This spatial covariance pattern should be evaluated further to determine whether it represents a biological marker of antidepressant treatment response and/or cognitive decline in LLD patients.

Translational Psychiatry (2021)11:473 ; <https://doi.org/10.1038/s41398-021-01539-9>

INTRODUCTION

Major depressive disorder in late-life is a risk factor for the development of all-cause dementia [1, 2]. Further, depressive symptoms are a risk factor for cognitive decline in cognitively normal individuals, as well as in individuals with mild cognitive impairment [3, 4]. The treatment of late-life depression (LLD) may be a target for dementia prevention [5, 6]. However, antidepressant treatments, developed for the treatment of younger patients, are effective in about half of patients in late-life [7]. The pathophysiology of LLD is multi-factorial and includes neurochemical, neurodegenerative and cerebrovascular disease mechanisms [8]. A clearer understanding of the neurobiology of LLD may facilitate the identification of individuals at risk for cognitive decline, as well as contribute to the development of more effective symptomatic treatments and strategies for prevention.

Molecular imaging studies of LLD have focused on Alzheimer's disease (AD) pathology, employing positron emission tomography

(PET) radiotracer imaging of beta-amyloid (A β), as well as fluid biomarkers [9–12]. PET studies have shown either no difference, higher or lower A β in LLD patients compared to healthy controls. When greater A β was observed in LLD patients than controls (in the absence of a mild cognitive impairment (MCI) or AD diagnosis), A β was detected in a more localized neuroanatomic distribution compared to MCI or AD [10, 13]. Studies in cognitively normal individuals have shown an association between depressive symptoms and greater A β and Tau [14, 15]. A β measured with PET and plasma CSF tau/A β 42 ratios was associated with the development of depressive symptoms in longitudinal studies of healthy controls [16, 17]. While there are discrepancies in the observation of greater A β in LLD patients, evidence suggests that in cognitively normal individuals, A β and depressive symptoms interact synergistically and are associated with cognitive decline [18].

While PET measures of A β and Tau show independent associations with cognitive deficits and cognitive decline in

¹Division of Geriatric Psychiatry and Neuropsychiatry, Department of Psychiatry and Behavioral Sciences, Johns Hopkins University School of Medicine, Baltimore, MD, USA.

²Division of Nuclear Medicine and Molecular Imaging, Russell H. Morgan Department of Radiology and Radiological Sciences, Johns Hopkins University School of Medicine, Baltimore, MD, USA. ³Banner Alzheimer's Institute, Phoenix, AZ, USA. ⁴Department of Pathology (Neuropathology), Johns Hopkins University School of Medicine, Baltimore, MD, USA.

⁵Division of Neuroradiology, Russell H. Morgan Department of Radiology and Radiological Sciences, Johns Hopkins University School of Medicine, Baltimore, MD, USA.

⁶Department of Genetic Medicine, Johns Hopkins University School of Medicine, Baltimore, MD, USA. ⁷These authors contributed equally: Gwenn S. Smith, Clifford I. Workman.

[✉]email: gsmith95@jhmi.edu

Received: 13 April 2021 Revised: 13 July 2021 Accepted: 26 July 2021

Published online: 13 September 2021

healthy controls and individuals with MCI, their predictive value is increased by including measures associated with neuronal dysfunction or degeneration (e.g., measures of cerebral glucose metabolism or gray matter volume) [19–22]. Studies comparing LLD patients to controls have demonstrated cortical and hippocampal atrophy and increased glucose metabolism in cortical regions that are hypometabolic both in AD patients and in individuals at genetic risk for AD [23–25]. To understand the neurobiology of LLD, multi-radiotracer imaging may provide information regarding AD pathology as well as detecting associated molecular mechanisms that have been implicated in both depression and neurodegenerative disease.

In considering molecular mechanisms associated with AD pathology, degeneration of monoamine systems (especially the serotonin system) has been observed in normal aging, MCI and AD, as well as depression [26, 27]. In AD, serotonergic deficits are greater and more widespread than deficits in other monoaminergic and cholinergic systems [28, 29]. Molecular imaging studies of the serotonin system have focused on measuring serotonin transporter availability (5-HTT). 5-HTT is a more specific marker of serotonin degeneration than serotonin receptors (e.g., 5-HT1a or 5-HT2a) as receptors are localized also on the terminals of non-serotonergic neurons [30]. Lower 5-HTT in depressed patients across the lifespan and in neurodegenerative diseases has been shown [31–33]. Modest decreases in 5-HTT have been observed in temporal cortical and limbic regions (amygdala, hippocampus) in LLD patients relative to controls, in contrast to the lack of a difference in serotonin receptor availability (5-HT1a and 5-HT2a) [32, 34, 35]. Lower 5-HTT has been observed also in patients with MCI and AD [33, 36].

The relationship between serotonin degeneration and AD pathology has been appreciated in preclinical studies. In a transgenic model of β -amyloidosis (APPswe/PS1dE9 mice), reduced serotonergic and noradrenergic fiber densities in the cortex and hippocampus were observed that occurred in parallel to the onset of deficits in episodic memory (12 months) and worsened at the onset of reference memory deficits and anxiety (18 months) [37]. Substantial cortical A β occurred later (18–24 months) at a time when cell loss in the subcortical monoaminergic nuclei (raphe nuclei, locus coeruleus) was observed. This pattern of monoamine degeneration was similar to that observed in AD [26]. Further analyses in this and similar transgenic amyloid mouse models showed loss of 5-HTT and 5-HT1b receptors, decreased serotonin release and an increase in the A β -related inflammatory response that was associated with change in these serotonergic markers [38, 39].

In the present study, the association between A β and 5-HTT in LLD patients and healthy controls was studied with PET imaging using well-characterized radiotracers for A β (N-methyl-[11C]2-(4'-methylaminophenyl)-6-hydroxybenzothiazole, [11C]-PiB) and for 5-HTT ([11C]-3-amino-4-(2-dimethylaminomethyl-phenylsulfanyl)-enzonitrile, [11C]-DASB) [40, 41]. The voxel-wise, multi-modal partial least square (mmPLS) analytic technique was applied to identify the spatial covariance pattern of A β and 5-HTT that maximally distinguished LLD patients from controls [42]. The hypotheses were tested that a spatial covariance pattern of higher A β and lower 5-HTT in frontal, temporal and parietal cortical regions would differentiate LLD patients from healthy controls. Greater expression of this pattern was predicted to correlate with greater depressive symptoms.

MATERIALS AND METHODS

Participant screening and selection

LLD patients were recruited from advertisements in the community. Controls were recruited from advertisements or from the Johns Hopkins University Alzheimer's Disease Research Center (2P50AG005146). To determine study eligibility, potential LLD patients and controls underwent

screening that included physical and neurological examination, laboratory testing and toxicology screening and psychiatric and neuropsychological evaluations. A Structured Clinical Interview for DSM-V was administered by a clinical psychologist (NG) [43], along with the antidepressant treatment history form [44], Clinical Dementia Rating scale (CDR) and a Mini Mental State Examination (MMSE) [45, 46]. LLD patients were enrolled if they were over age 60, had a DSM-V diagnosis of current major depressive episode (non-bipolar, non-psychotic) and a score of 17 or higher on the Hamilton Depression Rating Scale (HDRS) [47]. Participants were excluded from enrollment based on the following criteria: (1) a history of active neurological or Axis I psychiatric disorders (including dementia), except for a diagnosis of current major depressive episode (non-bipolar, non-psychotic) in the LLD patients; (2) not medically stable (i.e., poorly controlled medical conditions including hypertension and/or diabetes); (3) a positive toxicology screening and/or use of psychotropic drugs or medications with central nervous system effects (e.g., antihistamines, cold medications) within 2 weeks prior to enrollment and (4) contraindications for undergoing magnetic resonance imaging (MRI) scans (e.g., pacemaker, metal implants, aneurism clamps). The study protocol and consent forms were approved by the Institutional Review Board and the Radiation Research Committee of the Johns Hopkins University School of Medicine. Participants received both a transcribed and verbal description of the study and written informed consent was obtained.

Genotyping

Apolipoprotein E (APOE) genotyping was performed (in the laboratory of DA) using polymerase chain reaction amplification of genomic DNA digestion with HhaI restriction enzyme and gel electrophoresis, as described previously [48].

MR imaging procedures

MRI scans of the brain were acquired within a week before the PET scans at the F. M. Kirby Research Center for Functional Brain Imaging of the Kennedy Krieger Institute, as described previously [13, 32]. A Phillips 3.0 T Achieva MRI instrument was used with an 8-channel head coil (Phillips Medical Systems, Best, Netherlands). The magnetization-prepared rapid acquisition with gradient-echo (MPRAGE) pulse sequence (TE = 4, TR = 8.9, flip angle = 8 degrees, NSA = 1, 0.7 mm isotropic voxel size) was used for PET image processing.

PET imaging acquisition, quantification and preprocessing

PET scans were performed at the PET Center of the Russell H. Morgan Department of Radiology, Johns Hopkins University School of Medicine. The scanner used was a second-generation High Resolution Research Tomograph scanner (HRRT, Siemens Healthcare, Knoxville, TN), a cerium-doped lutetium oxyorthosilicate (Lu25i05 [Ce] or LSO) detector-based, dedicated brain PET scanner [49, 50]. The radiotracers [11C]-PiB and [11C]-DASB, used to measure A β and 5-HTT, respectively, were synthesized according to published methods [40, 41]. The PET scans were performed within 1 week of each other. Procedures for PET scan acquisition and reconstruction have been described previously [13, 32].

PET tracer kinetic modeling, image processing and statistical parametric mapping (SPM) analysis

Regional distribution volume ratio (DVR) values of [11C]-PiB were obtained by the multilinear reference tissue method with 2 parameters (MRTM2) [40, 51]. Regional DVR values of [11C]-DASB were obtained by the reference tissue graphical analysis method (RTGA) [32, 52, 53]. For both radiotracers, the cerebellar gray matter (excluding the vermis) was used as the reference region. The pre-processing of the parametric [11C]-PiB and [11C]-DASB DVR images was performed with SPM12 (SPM12; Institute of Neurology, London) as described previously [13, 32].

Multi-modal partial least squares (mmPLS)

In 2009, Chen and colleagues introduced the voxel-based, multi-modal application of the partial least square algorithm [42, 54]. The technique was applied to combine PET studies of cerebral glucose metabolism with structural MRI data to measure ApoE4 gene-dose effects in cognitively normal individuals [55]. These and other studies demonstrated the power of integrating information from different imaging modalities to increase statistical power and to address the issue of multiple comparisons associated with univariate, voxel-wise analyses. There are two types of

mmPLS: agnostic and informed mmPLS. In informed mmPLS, the variable of interest (e.g., diagnostic group membership) was directly incorporated into the mmPLS process. Agnostic mmPLS, on the other hand, is performed blind to the variable of interest. Corresponding to each of the two approaches, statistical test procedures were established to objectively assess type-I error related to the variable of interest (e.g., group differences). The algorithm generates images of the co-varying pattern for each modality and a single mmPLS score (subject score) for each person to reflect the strength of this co-varying pattern.

Agnostic mmPLS was used in this study, given that the primary interest was to assess between-group differences and relationship between the neuroimaging-based measures (mmPLS) and depressive symptom ratings. In running the agnostic mmPLS for dual-modality A β and 5-HTT PET data, the covariance patterns were estimated blindly over all subjects (no diagnostic group information was used). The between-group difference was tested using the subject scores associated with each of the spatial covariance patterns. First, agnostic mmPLS was run to generate the co-varying patterns between A β and 5-HTT. Then, between-group differences and correlations with depressive symptom ratings were evaluated using the subject scores from the mmPLS procedure that reflects the extent to which each subject expressed the spatial covariance pattern.

Statistical analysis

Between-group differences in the demographic and clinical measures were tested using analyses of variance (ANOVA) for interval variables, and Chi-square test for categorical variables. The general linear model in SPM12 examined voxel-wise group difference for each of the two PET radiotracers separately. To address the issue of multiple comparison correction, the Monte-Carlo simulation procedure developed by Chen and colleagues was applied to test the hypothesis that the number of between-group, voxel-wise differences in A β and 5-HTT in the predicted direction (greater A β and less 5-HTT in LLD patients than controls) was significantly greater than differences in the opposite direction. This is a method of estimating the overall significance of the entire voxel-wise image that is not influenced by the type I error associated with multiple regional comparisons. This method has been described previously and is similar to methods developed for voxel-based analyses of other neuroimaging modalities (e.g., structural magnetic resonance and Tau imaging) [56, 57]. Mean cortical A β values are reported as calculated previously [13].

The mmPLS spatial covariance pattern (as a 3D brain map) was scaled by the brain-map wide standard deviation within the search area to form the z-score map and was displayed with a threshold of $P=0.05$, as the correction for multiple comparisons is not relevant for the covariance spatial pattern display. Subject scores, which are free of the need for multiple comparisons corrections associated with voxel-wise, mmPLS analyses were generated blinded to group membership, were used to examine the group differences and to identify the related spatial covariance patterns. Realizing that the subject scores are paired, one for each PET radiotracer, group differences were initially examined using the multivariate Hotelling T square test. Realizing also, however, the close correlation between A β and 5-HTT for each subject score pair, principal component analysis (PCA) was applied to project the paired subject scores along the direction of the PCA major axis to form a single subject score to which the conventional univariate two-sample independent t test could be applied. The integrated univariate subject scores were also used to examine relationships with depression measures. Finally, if more than one spatial covariance pattern was associated with group differences, the formation of a single pattern was attempted by taking a weighted sum with the weights estimated by the general linear model, which included the subject scores of the corresponding patterns as the predictors to distinguish group membership. Brain regions were identified using the AAL and AAL3 atlases to localize significant results in the brainstem [58–60].

RESULTS

Twenty LLD patients and 20 healthy controls were enrolled in the study. The demographic characteristics, depression, cognitive and clinical measures are shown in Table 1. The groups did not differ significantly in age and sex distribution, years of education or cognitive functioning (MMSE or CDR sum of boxes). One of the controls and no LLD patients were left-handed. All controls received a CDR score of 0 (normal). All but one LLD patient

Table 1. Demographic and clinical characteristics of the late-life depressed (LLD) patients and controls.

	Healthy controls (<i>n</i> = 20)	LLD Patients (<i>n</i> = 20)
Age (years)	65 \pm 7	67 \pm 6
Sex (F/M)	10/10	10/10
Education (years)	15.5 \pm 4	16.5 \pm 2
MMSE	29 \pm 1	29 \pm 1
HDRS	1 \pm 1	18 \pm 2 ^a
BDI	2 \pm 3	24 \pm 8 ^b

MMSE modified Mini-Mental State Examination, BDI Beck Depression Inventory, HDRS Hamilton Depression Rating Scale.

^aSignificant between group difference ($F(1,39) = 879.3, P < 0.001$).

^bSignificant between group difference ($F(1,39) = 149.4, P < 0.001$).

received a CDR score of 0. This patient received a score of 0.5 (MCI: sum of boxes = 1.5 for memory, orientation, judgment and problem-solving subscales). Another patient received a CDR of 0 and a sum of boxes = 0.5 (judgment and problem-solving subscale). In addition, groups were comparable in the number of ApoE4 alleles (1 subject was a homozygote and 3 subjects were heterozygotes in each group). As expected, LLD patients showed significantly higher HDRS and BDI scores than controls ($F(1,39) = 879.3, P < 0.001$); $F(1,39) = 149.4, P < 0.001$, respectively, within a range of moderate to moderate-to-severe depressive symptoms, respectively. All patients had one prior depressive episode not including the present episode (5 patients with onset before age 65 and 15 patients with onset after age 65). The age at onset of depression was 58 \pm 11 years (range 33–75 years) and the duration of the present episode was 14 \pm 10 months (range 2–36 months). None of the LLD patients were taking psychotropic drugs at the time of scanning, including antidepressants, antipsychotics and mood stabilizers. Three LLD patients were treated previously with an adequate trial of selective serotonin reuptake inhibitors (SSRIs) in late life, although not within 2 years of enrollment in the study. The number of participants who were taking medications to treat the following medical co-morbidities were: hypertension (7 control/6 patients), cholesterol lowering medications (6 control/6 patients) and oral anti-diabetogenic agents (0 control/2 patients), but none were taking insulin. No patients had pulmonary disease requiring treatment.

Unimodal, univariate SPM results

SPM12 based voxel-wise analyses were performed separately for A β and 5-HTT to examine the group differences between normal controls and LLD patients (Fig. 1, Table 2). For each unimodal SPM voxel-wise analysis, none of the regions survived multiple comparison correction using the commonly reported height threshold $p = 0.001$ and cluster-level threshold of FDR at $P > 0.05$. When examining the omnibus significance using Monte-Carlo simulation, there were 21842 voxels where 5-HTT availability was lower in LLD patients compared to controls, while there were only 3877 voxels in the opposite direction. Using the Monte-Carlo simulation over 1000 runs, the omnibus significance for 5-HTT was $P < 0.002$. Similarly, the omnibus significance was $P < 0.001$ for A β for which 22591 and 4582 voxels were observed where A β DVR was higher and lower, respectively in LLD patients compared to controls. At a peak-voxel uncorrected threshold of $P = 0.005$, 5-HTT was lower in LLD patients compared to controls superior temporal pole (left), inferior temporal gyrus (right), parahippocampal gyrus (right), fusiform (bilateral), amygdala (bilateral), dorsal, medial and pontine raphe nuclei. A β was higher in LLD patients compared to controls in middle frontal gyrus (left), superior and inferior parietal gyrus (left), precuneus (left), angular

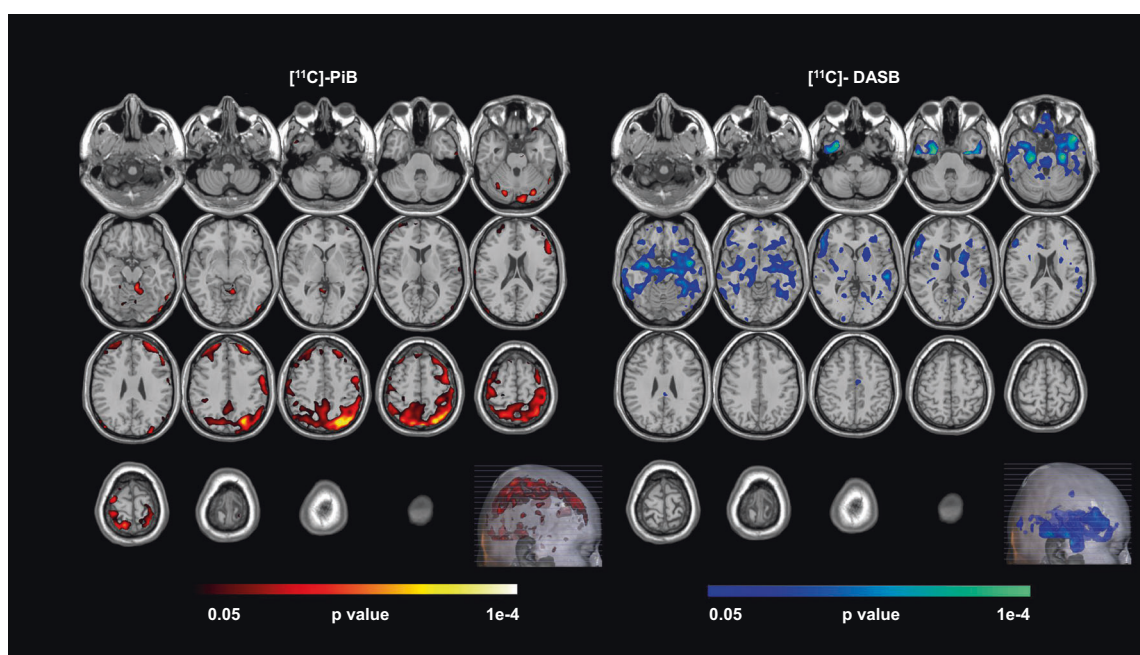


Fig. 1 Voxel-wise, statistical parametric mapping (version 12) unimodal analysis for [^{11}C]-PiB and [^{11}C]-DASB, separately. Higher beta-amyloid (left, hot colored areas) and lower serotonin transporter availability (right, cool colored areas) was observed in Late-Life Depressed (LLD) Patients than in normal controls, applying the Monte-Carlo Simulation Method (uncorrected $P = 0.005$).

Table 2. Peak voxel locations identified by statistical parametric mapping (version 12) unimodal analysis.

Brain region	Hemisphere	Atlas coordinates millimeters (MNI) X Y Z	P value
Greater beta-amyloid burden in LLD patients compared to controls			
Middle Frontal Gyrus	Left	-28 50 36	9.0E-04
Superior Parietal Gyrus	Left	-26 -74 56	5.4E-04
Precuneus	Left	-4 -80 56	1.3E-03
Inferior Parietal Gyrus	Left	-26 -72 44	3.3E-04
Angular Gyrus	Left	-40 -72 48	4.9E-04
Superior Occipital Gyrus	Left	-26 -72 40	4.0E-04
Lower 5-HTT in LLD patients compared to controls			
Parahippocampal Gyrus	Right	28 -28 -32	2.1E-05
Superior Temporal Pole	Left	-48 14 -24	7.6E-05
Inferior Temporal Gyrus	Right	32 2 -44	1.8E-04
Amygdala	Right	30 -6 -14	4.02E-04
Amygdala	Left	-26 2 -26	1.9E-03
Fusiform Gyrus	Right	30 -12 -36	1.3E-05
Fusiform Gyrus	Left	-28 -12 -32	1.8E-04
Raphe Pontine		-6 -18 -20	6.3E-03
Raphe Median		0 -30 -24	1.3E-02
Raphe Dorsal		4 -28 -12	3.4E-02

Higher Beta-Amyloid (top section) and lower serotonin transporter availability (bottom section) was observed in Late-Life Depressed (LLD) Patients than normal controls, applying the Monte-Carlo Simulation Method (uncorrected $P = 0.005$).

gyrus (left) and superior occipital gyrus (left). The mean A β DVRs for the total cortex and the left precuneus were 1.13 ± 0.63 and 1.24 ± 0.09 for the controls and 1.17 ± 0.16 and 1.31 ± 0.24 for the LLD patients based on volume of interest analysis [13].

Dual-modal agnostic mmPLS results

Two patterns were identified that showed significant group differences based on the integrated subject score (the main PCA component for the A β subject score and 5-HTT subject score, t

(2,37) = -2.637; $P = 0.012$; t (2,37) = -2.110; $P = 0.046$, respectively). To further reduce the possibility of type-I error, the two patterns were combined via the general linear model with the corresponding subject scores as the independent predictors for group differences. The distribution of subject scores for the two groups is shown in Fig. 2. The subject scores are significantly lower in the LLD group than the normal control group (t (2,37) = -3.623; $P = 0.0009$) when subject scores for A β and 5-HTT were further integrated using PCA. The combined spatial covariance pattern for

the two groups and the peak voxel locations for the between-group differences are shown in Fig. 3 and Table 3, respectively. Note that this spatial covariance pattern display is not for statistical inference and there is no need for the correction of multiple comparisons. The combined component demonstrated an association between decreased 5-HTT in the putamen (bilateral), thalamus (bilateral), hippocampus (left), amygdala (bilateral), dorsal, medial and pontine raphe nuclei and higher A β in the inferior temporal gyrus (left), precuneus (right), inferior parietal gyrus (left), superior occipital gyrus (right) and cuneus (right).

Correlation results

In addition to the blinded group membership information, the mmPLS pipeline was also agnostic to the depression severity measures. Using the same mmPLS integrated and modality-specific subject scores, the relationship between mmPLS spatial

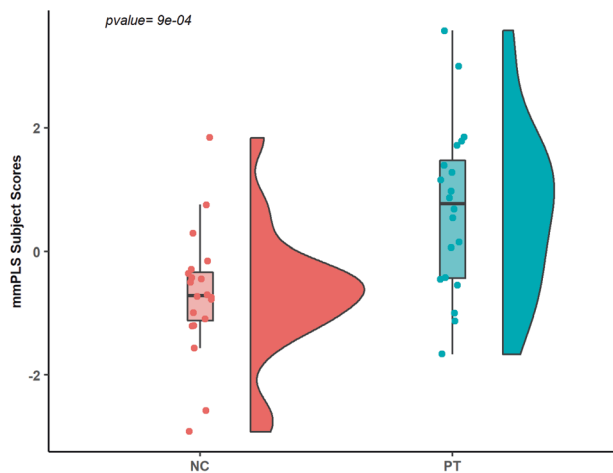


Fig. 2 Subject scores for normal controls (NC) and late-life depressed (PT) patients. Subject scores determined by multi-modal partial least squares.

covariance pattern and the depression measures were examined. For all subjects combined, greater expression of the 5-HTT and A β covariance pattern was correlated with greater depressive symptoms (Hamilton Depression Rating Scale Score) (HDRS: $r_s =$

Table 3. The peak voxel locations of the co-varying spatial patterns of Greater Beta-Amyloid and the Serotonin Transporter (5-HTT) determined by multi-modal Partial Least Squares (mmPLS) for the Normal Controls and Late-Life Depressed Patient Groups.

Brain region	Hemisphere	Atlas coordinates millimeters (MNI) X Y Z	P value
Greater beta-amyloid in LLD patients compared to controls			
Inferior Temporal Gyrus	Left	-58 -54 -24	2.0E-05
Precuneus	Right	6 -78 52	7.1E-06
Precuneus	Right	6 -78 56	2.2E-05
Inferior Parietal Gyrus	Left	-32 -68 44	8.6E-04
Superior Occipital Gyrus	Right	22 -78 40	1.5E-07
Cuneus	Right	14 -76 36	7.8E-06
Lower 5-HTT in LLD patients compared to controls			
Putamen	Right	26 -4 -4	5.6E-05
Putamen	Left	-22 12 -4	3.7E-05
Thalamus	Right	14 -28 0	9.0E-09
Thalamus	Left	-12 -28 4	1.4E-05
Amygdala	Right	28 -6 -14	2.4E-04
Amygdala	Left	-26 -8 -12	7.7E-05
Hippocampus	Left	-26 -8 -16	3.1E-04
Pontine Raphe		-2 -26 -20	3.1E-07
Dorsal Raphe		0 -28 -14	8.2E-18
Median Raphe		0 -30 -20	1.6E-09

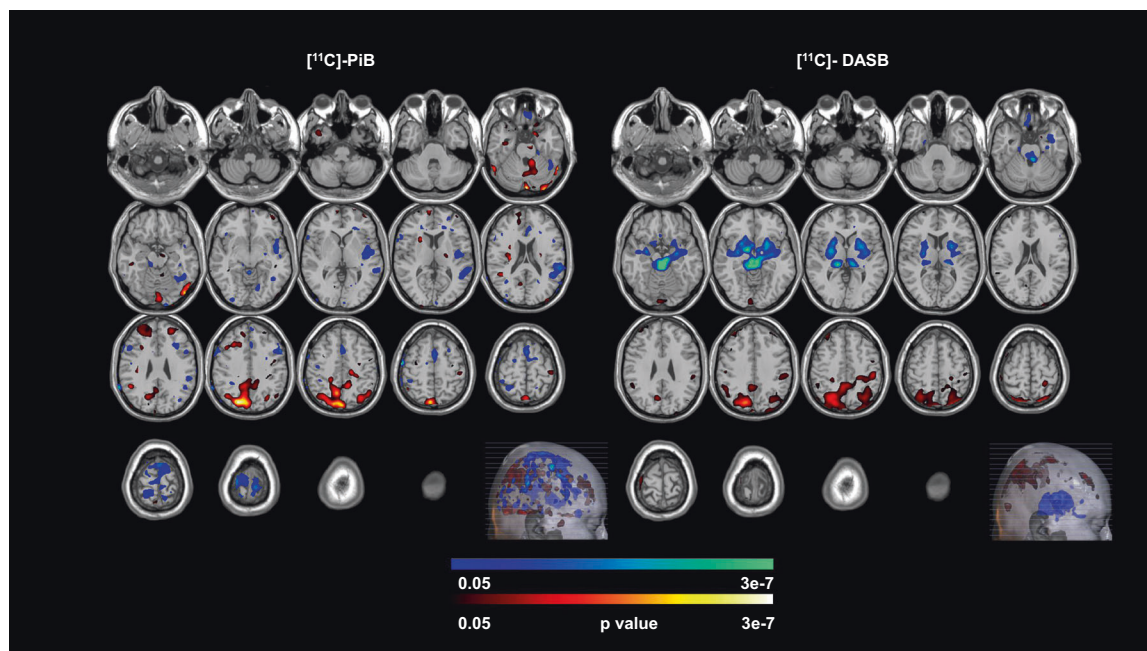


Fig. 3 Co-varying spatial patterns between beta-amyloid deposition and serotonin transporter availability. Covarying Spatial patterns determined by Multi-Modal Partial Least Squares in normal controls and late-lifedepressed patients.

Table 4. Correlation between multi-modal partial least squares (mmPLS) determined subject scores and depression severity.

Depression Measure	Integrated		Beta-amyloid		Serotonin transporter availability	
	R_s	<i>P</i> value	R_s	<i>P</i> value	R_s	<i>P</i> value
Hamilton Depression Rating Scale	0.43	0.006	0.50	0.001	0.35	0.03
Beck Depression Inventory	0.44	0.005	0.45	0.003	0.42	0.007

0.43; $P = 0.006$) and Beck Depression Inventory (BDI $r_s = 0.44$; $P = 0.005$; Table 4). The correlation of depressive symptoms with A β and 5-HTT were similar (A β : $r_s = 0.50$; $P = 0.001$ and $r_s = 0.45$; $P = 0.003$ and 5-HTT: $r_s = 0.35$; $P = 0.03$ and $r_s = 0.42$; $P = 0.007$) with HDRS and BDI, respectively. As the mmPLS method is designed to identify the maximal covariance of two spatial patterns, the A β and 5-HTT patterns are not entirely independent and the correlations are expected to be similar.

DISCUSSION

A spatial covariance pattern of lower 5-HTT and higher A β was identified that distinguished LLD patients from controls. Specifically, lower 5-HTT in striatal, thalamic (anterior and medial-dorsal nuclei), limbic (amygdala and hippocampus) and raphe nuclei (dorsal, medial, and pontine) were associated with greater A β in temporal, parietal and occipital regions. Greater expression of the combined pattern, as well as both A β and 5-HTT patterns, was correlated with greater depressive symptoms. Most prior studies have not observed a correlation between depressive symptoms and 5-HTT availability [31]. The correlation between depressive symptoms and 5-HTT pattern may have been significant in the present study because the 5-HTT pattern is not entirely independent of A β using this analysis method. The cortical distribution of A β in the LLD patients is less in magnitude and extent as compared to the distribution of A β in patients with MCI or AD and is similar to other studies in which higher A β was observed in LLD patients relative to controls [10, 61, 62]. Importantly, significant associations between the two radiotracers were observed that discriminate between control and LLD groups, while robust between group differences in A β and 5-HTT were only observed when examining the omnibus global significance for analyzing each radiotracers separately. Based on the omnibus global assessment of significance, overall higher A β and lower 5-HTT density was detected in LLD patients as compared to healthy controls, while the conventional voxel-based comparisons (SPM12), using a stringent statistical threshold, did not detect localized between-group differences. Previous exploratory voxel-wise analyses showed similar results for A β and 5-HTT [13, 32]. Although the unimodal approach could not evaluate associations between neurobiological processes, mmPLS, revealed associations between the degree of regional A β and 5-HTT.

Several aspects of the spatial covariance pattern are noteworthy. At this relatively early stage of A β , decreases in 5-HTT are observed. The raphe nuclei and subcortical and limbic regions are among regions with the highest concentration of 5-HTT in the brain [63, 64]. The raphe nuclei include the cell bodies that synthesize serotonin and are the origin of serotonin innervation throughout the brain [63]. The critical role of serotonin is underscored by the dense serotonin innervation throughout the CNS and the observation in the rat brain that every cell in the cortex is in close proximity to a serotonin containing neuron [63]. The spatial covariance pattern did not include cortical 5-HTT, even though neurodegeneration of the raphe nuclei (suggested by the loss of 5-HTT) would be expected to have a widespread influence on cortical serotonin. 5-HTT may not be sensitive to detecting cortical serotonin dysfunction due to its relatively lower

concentration in cortex than the other regions included in the pattern. In contrast, a study in Parkinson's Disease (PD) patients showed a correlation between higher cortical A β and lower cortical 5-HTT and between higher cortical A β and lower midbrain 5-HTT. However, the levels of cortical A β in the PD patients in this study were comparable to the LLD patients in the present study [65]. A further understanding of the longitudinal regional-specific associations may be critical in understanding mechanisms of LLD and antidepressant response, as well as cognitive decline.

While the present results do not imply causality and may represent two-co-occurring pathologies, interventions targeting either A β or 5-HTT have an effect on the other pathology. A β immunotherapies show a protective effect on the serotonin system, while interventions for multiple serotonergic targets show a reduction in AD pathology. A β immunization attenuated both A β and serotonin degeneration in transgenic mice (APPswe/PS1dE9) [66]. Early SSRI treatment prevented the development of AD pathology (A β and/or Tau), spatial memory deficits and depression-like symptoms in amyloid (APPswe/PS1dE9) and triple-transgenic mouse models (3xTg-AD) [67, 68]. In the APP/presenilin 1 mouse model and in healthy human subjects, the antidepressant Escitalopram reduced interstitial fluid A β and CSF A β 42 level, respectively [69, 70]. Serotonergic receptor modulators (such as 5-HT4 agonists, 5-HT6 antagonists) that have antidepressant effects reduced A β [71, 72]. Importantly, preclinical studies show that serotonergic agents have multiple mechanisms relevant to prevention and symptomatic treatment of both depression and cognitive deficits, in addition to blocking A β and Tau, neuroprotection and synaptic plasticity [73]. Thus, an understanding of the role of the serotonin system in relation to AD pathology in LLD may have implications for symptomatic treatment and prevention.

In conclusion, the present study focused on evaluating A β relative to a molecular mechanism that is associated with depressive disorders and cognitive deficits and has been linked to A β in preclinical studies, serotonin degeneration as reflected by loss of 5-HTT [32, 33, 37]. Using mmPLS, unique associations between A β and 5-HTT were demonstrated in LLD patients relative to controls. The results suggest that mmPLS can be applied to understand the synaptic changes potentially associated with A β , especially at a relatively early stage of A β . The evaluation of 5-HTT in relation to A β in a larger, more heterogeneous LLD patient sample would determine whether the spatial covariance pattern may be a sensitive biomarker to identify LLD patients who may respond poorly to SSRI treatment or who may be "at risk" for cognitive decline.

REFERENCES

- Byers AL, Yaffe K. Depression and risk of developing dementia. *Nat Rev Neurol*. 2011;7:323–31. <https://doi.org/10.1038/nrneurol.2011.60>
- Diniz BS, Butters MA, Albert SM, Dew MA, Reynolds CF. Late-life depression and risk of vascular dementia and Alzheimer's disease: systematic review and meta-analysis of community-based cohort studies. *Br J Psychiatry*. 2013;202:329–35. <https://doi.org/10.1192/bjp.bp.112.118307>. Published online
- Modrego PJ, Ferrández J. Depression in patients with mild cognitive impairment increases the risk of developing dementia of Alzheimer type: a prospective cohort study. *Arch Neurol*. 2004;61:1290–3. <https://doi.org/10.1001/archneur.61.8.1290>. Published online

4. Barnes DE, Yaffe K, Byers AL, McCormick M, Schaefer C, Whitmer RA. Midlife vs late-life depressive symptoms and risk of dementia. *Arch Gen Psychiatry*. 2012;69:493–8. <https://doi.org/10.1001/archgenpsychiatry.2011.1481>
5. Livingston G, Sommerlad A, Orgeta V, Costafreda SG, Huntley J, Ames D, et al. Dementia prevention, intervention, and care. *Lancet*. 2017;390:2673–734. [https://doi.org/10.1016/S0140-6736\(17\)31363-6](https://doi.org/10.1016/S0140-6736(17)31363-6). Published online
6. Dafsari FS, Jessen F. Depression—an underrecognized target for prevention of dementia in Alzheimer's disease. *Transl Psychiatry*. 2020;10:160 <https://doi.org/10.1038/s41398-020-0839-1>. Published online
7. Smith GS, Gunning-Dixon FM, Lotrich FE, Taylor WD, Evans JD. Translational research in late-life mood disorders: Implications for future intervention and prevention research. *Neuropsychopharmacology*. 2007;32:1857–75. <https://doi.org/10.1038/sj.npp.1301333>. Published online
8. Butters MA, Young JB, Lopez O, Aizenstein HJ, Mulsant BH, Reynolds CF 3rd, et al. Pathways linking late-life depression to persistent cognitive impairment and dementia. *Dialogues Clin Neurosci*. 2008;10:345–57. <https://doi.org/10.31887/DCNS.2008.10.3/mabutters>.
9. Butters MA, Klunk WE, Mathis CA, Price JC, Ziolk SK, Hoge JA, et al. Imaging Alzheimer pathology in late-life depression with PET and Pittsburgh compound-B. *Alzheimer Dis Assoc Disord*. 2008;22:261–8. <https://doi.org/10.1097/WAD.0b013e31816c92bf>. Published online
10. Kumar A, Kepe V, Barrio JR, Siddarth P, Manoukian V, Elderkin-Thompson V, et al. Protein binding in patients with late-life depression. *Arch Gen Psychiatry*. 2011;68:1143–50. <https://doi.org/10.1001/archgenpsychiatry.2011.122>. Published online
11. Mackin RS, Insel PS, Landau S, Bickford D, Morin R, Rhodes E, et al. Late-life depression is associated with reduced cortical amyloid burden: findings from the Alzheimer's disease neuroimaging initiative depression project. *Biol Psychiatry*. 2020;89:757–65. <https://doi.org/10.1016/j.biopsych.2020.06.017>. Published online
12. Fiaux do Nascimento KK, Pereira KS, Satler S, Diniz B, Malloy-Diniz LF, Butters M. Plasma and cerebrospinal fluid amyloid- β levels in late-life depression: a systematic review and meta-analysis. *Alzheimer's Dement*. 2015;11:P655 <https://doi.org/10.1016/j.jalz.2015.06.959>. Published online
13. Smith GS, Kuwabara H, Nandi A, Gould NF, Nassery N, Savonenko A, et al. Molecular imaging of beta-amyloid deposition in late-life depression. *Neurobiol Aging*. 2021;101:85–93. <https://doi.org/10.1016/j.neurobiolaging.2021.01.002>.
14. Gatchel JR, Donovan NJ, Locascio JJ, Schultz AP, Becker JA, Chhatwal J, et al. Depressive symptoms and tau accumulation in the inferior temporal lobe and entorhinal cortex in cognitively normal older adults: a pilot study. *J Alzheimer's Dis*. 2017;59:975–85. <https://doi.org/10.3233/JAD-170001>. Published online
15. Gatchel JR, Rabin JS, Buckley RF, Locascio JJ, Quiroz YT, Yang HS, et al. Longitudinal association of depression symptoms with cognition and cortical amyloid among community-dwelling older adults. *JAMA Netw Open*. 2019;2:198964 <https://doi.org/10.1001/jamanetworkopen.2019.8964>. Published online
16. Babulal GM, Ghoshal N, Head D, Vernon EK, Holtzman DM, Benzinger T, et al. Mood changes in cognitively normal older adults are linked to Alzheimer disease biomarker levels. *Am J Geriatr Psychiatry*. 2016;24:1095–104. <https://doi.org/10.1016/j.jagp.2016.04.004>. Published online
17. Donovan NJ, et al. Longitudinal association of amyloid beta and anxious-depressive symptoms in cognitively normal older adults. *Am J Psychiatry*. Published online 2018. <https://doi.org/10.1176/appi.ajp.20177040442>
18. Sperling RA, Mormino EC, Schultz AP, Betensky RA, Papp KV, Amariglio RE, et al. The impact of amyloid-beta and tau on prospective cognitive decline in older individuals. *Ann Neurol*. 2019;85:181–93. <https://doi.org/10.1002/ana.25395>. Published online
19. Mormino EC, Kluth JT, Madison CM, Rabinovici GD, Baker SL, Miller BL, et al. Episodic memory loss is related to hippocampal-mediated β -amyloid deposition in elderly subjects. *Brain*. 2009;132:1310–23. <https://doi.org/10.1093/brain/awn320>. Published online
20. Jack CR Jr, Lowe VJ, Weigand SD, Wiste HJ, Senjem ML, Knopman DS, et al. Serial PIB and MRI in normal, mild cognitive impairment and Alzheimer's disease: implications for sequence of pathological events in Alzheimer's disease. *Brain*. 2009;132:1355–65. <https://doi.org/10.1093/brain/awp062>. Published online
21. Brier MR, Gordon B, Friedrichsen K, McCarthy J, Stern A, Christensen J, et al. Tau and Ab imaging, CSF measures, and cognition in Alzheimer's disease. *Sci Transl Med*. 2016;8:338 <https://doi.org/10.1126/scitranslmed.aaf2362>. Published online
22. Jagust W. Is amyloid- β harmful to the brain? Insights from human imaging studies. *Brain*. 2016;139:23–30. <https://doi.org/10.1093/brain/aww326>. Published online
23. Jamieson A, Goodwill AM, Termine M, Campbell S, Szoek C. Depression related cerebral pathology and its relationship with cognitive functioning: a systematic review. *J Affect Disord*. 2019;250:410–8. <https://doi.org/10.1016/j.jad.2019.03.042>
24. Smith, GS, Kramer E, Ma Y, Kingsley P, Dhawan V, Chaly T, et al. The functional neuroanatomy of geriatric depression. *Int J Geriatr Psychiatry*. 2009;24. <https://doi.org/10.1002/gps.2185>
25. Reiman EM, Caselli RJ, Yun LS, Chen K, Bandy D, Minoshima S, et al. Preclinical evidence of Alzheimer's disease in persons homozygous for the $\epsilon 4$ allele for apolipoprotein E. *N Engl J Med*. 1996;334:752–8. <https://doi.org/10.1056/NEJM199603213341202>. Published online
26. Trillo L, Das D, Hsieh W, Medina B, Moghadam S, Lin B, et al. Ascending monoaminergic systems alterations in Alzheimer's disease. Translating basic science into clinical care. *Neurosci Biobehav Rev*. 2013;37:1363–79. <https://doi.org/10.1016/j.neubiorev.2013.05.008>. Published online
27. Underwood MD, Kassir SA, Bakalian MJ, Galfalvy H, Dwork AJ, Mann JJ, et al. Serotonin receptors and suicide, major depression, alcohol use disorder and reported early life adversity. *Transl Psychiatry*. 2018;8:279 <https://doi.org/10.1038/s41398-018-0309-1>. Published online
28. Palmer AM, Stratmann GC, Procter AW, Bowen DM. Possible neurotransmitter basis of behavioral changes in Alzheimer's disease. *Ann Neurol*. 1988;23:616–20. <https://doi.org/10.1002/ana.410230616>. Published online
29. Cross AJ, Crow TJ, Ferrier IN, Johnson JA. The selectivity of the reduction of serotonin 52 receptors in Alzheimer-type dementia. *Neurobiol Aging*. 1986;7:3–7. [https://doi.org/10.1016/0197-4580\(86\)90019-9](https://doi.org/10.1016/0197-4580(86)90019-9). Published online
30. Azmitia EC, Nixon R. Dystrophic serotonergic axons in neurodegenerative diseases. *Brain Res*. 2008;1217:185–94. <https://doi.org/10.1016/j.brainres.2008.03.060>. Published online
31. Spies M, Knudsen GM, Lanzenberger R, Kasper S. The serotonin transporter in psychiatric disorders: Insights from PET imaging. *Lancet Psychiatry*. 2015;2:743–55. [https://doi.org/10.1016/S2215-0366\(15\)00232-1](https://doi.org/10.1016/S2215-0366(15)00232-1)
32. Smith GS, Kuwabara H, Gould NF, Nassery N, Savonenko A, Joo JH, et al. Molecular imaging of the serotonin transporter availability and occupancy by antidepressant treatment in late-life depression. *Neuropharmacology*. 2021;194:108447. <https://doi.org/10.1016/j.neuropharm.2021.108447>.
33. Smith GS, Barrett FS, Joo JH, Nassery N, Savonenko A, Sodums DJ, et al. Molecular imaging of serotonin degeneration in mild cognitive impairment. *Neurobiol Dis*. 2017;105:33–41. <https://doi.org/10.1016/j.nbd.2017.05.007>.
34. Meltzer CC, Price JC, Mathis CA, Butters MA, Ziolk SK, Moses-Kolko E, et al. Serotonin 1A receptor binding and treatment response in late-life depression. *Neuropsychopharmacology*. 2004;29:2258–65. <https://doi.org/10.1038/sj.npp.1300556>. Published online
35. Meltzer CC, Price JC, Mathis CA, Greer PJ, Cantwell MN, Houck PR, et al. PET imaging of serotonin type 2A receptors in late-life neuropsychiatric disorders. *Am J Psychiatry*. 1999;156:1871–8. <https://doi.org/10.1176/ajp.156.12.1871>. Published online
36. Ouchi Y, Yoshikawa E, Futatsubashi M, Yagi S, Ueki T, Nakamura K. Altered brain serotonin transporter and associated glucose metabolism in Alzheimer disease. *J Nucl Med*. 2009;50:1260–6. <https://doi.org/10.2967/jnumed.109.063008>. Published online
37. Liu Y, Yoo MJ, Savonenko A, Stirling W, Price DL, Borchelt DR, et al. Amyloid pathology is associated with progressive monoaminergic neurodegeneration in a transgenic mouse model of Alzheimer's disease. *J Neurosci*. 2008;28:13805–14. <https://doi.org/10.1523/JNEUROSCI.4218-08.2008>
38. Tajeddinn W, Persson T, Maioli S, Calvo-Garrido J, Parrado-Fernandez C, Yoshitake T, et al. 5-HT1B and other related serotonergic proteins are altered in APPsw mutation. *Neurosci Lett*. 2015;594:137–43. <https://doi.org/10.1016/j.neulet.2015.03.064>. Published online
39. Metaxas A, Anzalone M, Vaitheeswaran R, Petersen S, Landau AM, Finsen B. Neuroinflammation and amyloid-beta 40 are associated with reduced serotonin transporter (SERT) activity in a transgenic model of familial Alzheimer's disease. *Alzheimer's Res Ther*. 2019;11:38 <https://doi.org/10.1186/s13195-019-0491-2>. Published online
40. Klunk WE, Engler H, Nordberg A, Wang Y, Blomqvist G, Holt DP, et al. Imaging brain amyloid in Alzheimer's disease with Pittsburgh compound-B. *Ann Neurol*. 2004;55:306–19. <https://doi.org/10.1002/ana.20009>
41. Wilson AA, Ginovart N, Hussey D, Meyer J, Houle S. In vitro and in vivo characterization of [^{11}C]-DASB: A probe for in vivo measurements of the serotonin transporter by positron emission tomography. *Nucl Med Biol*. 2002;29:509–15. [https://doi.org/10.1016/S0969-8051\(02\)00316-5](https://doi.org/10.1016/S0969-8051(02)00316-5)
42. Chen K, Reiman EM, Huan Z, Caselli RJ, Bandy D, Ayutyanont N, et al. Linking functional and structural brain images with multivariate network analyses: a novel application of the partial least square method. *Neuroimage*. 2009;47:602–10. <https://doi.org/10.1016/j.neuroimage.2009.04.053>
43. First MB, Spitzer RL, Gibbon M, Williams JBW. Structured Clinical Interview for DSM-IV Axis I Disorders-Patient Edition (SCID-I/P, Version 2.0) Vol. 1995 Biometrics Research Department, New York State Psychiatric Institute; New York <https://doi.org/10.1521/pe.1995.9.2.92>
44. Sackeim HA. The definition and meaning of treatment-resistant depression. *J Clin Psychiatry*. 2001;62 Suppl 16:10–7.
45. Morris JC. The clinical dementia rating (cdr): current version and scoring rules. *Neurol*. 1993;43:2412–4. <https://doi.org/10.1212/wnl.43.11.2412-a>

46. Folstein MF, Folstein SE, McHugh PR. "Mini-mental state". A practical method for grading the cognitive state of patients for the clinician. *J Psychiatr Res*. 1975;12:189–98. [https://doi.org/10.1016/0022-3956\(75\)90026-6](https://doi.org/10.1016/0022-3956(75)90026-6). Published online
47. Hamilton M. A rating scale for depression. *J Neurol Neurosurg Psychiatry*. 1960; 23:56–62.; 1959.
48. Avramopoulos D, Mikkelsen M, Vassilopoulos D, Grigoriadou M, Petersen MB. Apolipoprotein E allele distribution in parents of Down's syndrome children. *Lancet*. 1996;347:862–5. [https://doi.org/10.1016/S0140-6736\(96\)91346-X](https://doi.org/10.1016/S0140-6736(96)91346-X). Published online
49. Rahmim A, Cheng JC, Blinder S, Camborde ML, Sossi V. Statistical dynamic image reconstruction in state-of-the-art high-resolution PET. *Phys Med Biol*. 2005;50:4887–912. <https://doi.org/10.1088/0031-9155/50/20/010>. Published online
50. Sossi HWAM, de Jong WC, Barker P, Bloomfiel Z, Burbar M-L, Camborde C, et al. The second generation HRRT - A multi-centre scanner performance investigation. In: *IEEE Nuclear Science Symposium Conference Record*; 2005. <https://doi.org/10.1109/NSSMIC.2005.1596770>
51. Ichise M, Toyama H, Innis RB, Carson RE. Strategies to improve neuroreceptor parameter estimation by linear regression analysis. *J Cereb Blood Flow Metab*. 2002;22:1271–81. <https://doi.org/10.1097/00004647-200210000-00015>. Published online
52. Logan J, Fowler JS, Volkow ND, Wang GJ, Ding YS, Alexoff DL. Distribution volume ratios without blood sampling from graphical analysis of PET data. *J Cereb Blood Flow Metab*. 1996;16:834–40. <https://doi.org/10.1097/00004647-199609000-00008>. Published online
53. Innis RB, Cunningham VJ, Delforge J, Fujita M, Gjedde A, Gunn RN, et al. Consensus nomenclature for in vivo imaging of reversibly binding radioligands. *J Cereb Blood Flow Metab*. 2007;27:1533–9. <https://doi.org/10.1038/sj.jcbfm.9600493>. Published online
54. McIntosh AR, Bookstein FL, Haxby JV, Grady CL. Spatial pattern analysis of functional brain images using partial least squares. *Neuroimage*. 1996;3:143–57. <https://doi.org/10.1006/nimg.1996.0016>. Published online
55. Chen K, Ayutyanont N, Langbaum JB, Fleisher AS, Reschke C, Lee W, et al. Correlations between FDG PET glucose uptake-MRI gray matter volume scores and apolipoprotein E $\epsilon 4$ gene dose in cognitively normal adults: a cross-validation study using voxel-based multi-modal partial least squares. *Neuroimage*. 2012;60:2316–22. <https://doi.org/10.1016/j.neuroimage.2012.02.005>. Published online
56. Chen K, Reiman EM, Alexander GE, Bandy D, Renaut R, Crum WR, et al. An automated algorithm for the computation of brain volume change from sequential MRIs using an iterative principal component analysis and its evaluation for the assessment of whole-brain atrophy rates in patients with probable Alzheimer's disease. *Neuroimage*. 2004;22:134–43. <https://doi.org/10.1016/j.neuroimage.2004.01.002>. Published online
57. Stern RA, Adler CH, Chen K, Navitsky M, Luo J, Dodick DW, et al. Tau positron-emission tomography in Former National Football League Players. *N Engl J Med*. 2019;380:1716–25. <https://doi.org/10.1056/nejmoa1900757>. Published online
58. Tzourio-Mazoyer N, Landeau B, Papathanassiou D, Crivello F, Etard O, Delcroix N, et al. Automated anatomical labeling of activations in SPM using a macroscopic anatomical parcellation of the MNI MRI single-subject brain. *Neuroimage*. 2002;15:273–89. <https://doi.org/10.1006/nimg.2001.0978>. Published online
59. Rolls ET, Joliot M, Tzourio-Mazoyer N. Implementation of a new parcellation of the orbitofrontal cortex in the automated anatomical labeling atlas. *Neuroimage*. 2015;122:1–5. <https://doi.org/10.1016/j.neuroimage.2015.07.075>. Published online
60. Rolls ET, Huang CC, Lin CP, Feng J, Joliot M. Automated anatomical labelling atlas 3. *Neuroimage*. 2020;206:116189 <https://doi.org/10.1016/j.neuroimage.2019.116189>. Published online
61. Rabinovici GD, Jagust WJ. Amyloid imaging in aging and dementia: testing the amyloid hypothesis in vivo. *Behav Neurol*. 2009;21:117–28. <https://doi.org/10.3233/BEN-2009-0232>. Published online
62. McKee AC, Au R, Cabral HJ, Kowall NW, Seshadri S, Kubilus CA, et al. Visual association pathology in preclinical Alzheimer disease. *J Neuropathol Exp Neurol*. 2006;65:621–30. <https://doi.org/10.1097/00005072-200606000-00010>.
63. Molliver ME. Serotonergic neuronal systems: what their anatomic organization tells us about function. *J. Clin. Psychopharmacol*. 1987;7:3 <https://doi.org/10.1097/00004714-198712001-00002>. Published online
64. Várnäs K, Halldin C, Hall H. Autoradiographic distribution of serotonin transporters and receptor subtypes in human brain. *Hum. Brain Mapp*. 2004;22:246–60. <https://doi.org/10.1002/hbm.20035>.
65. Kotagal V, Spino C, Bohnen NI, Koeppe R, Albin RL. Serotonin, β -amyloid, and cognition in Parkinson disease. *Ann Neurol*. 2018;83:994–1002. <https://doi.org/10.1002/ana.25236>
66. Liu Y, Lee MK, James MM, Price DL, Borchelt DR, Troncoso JC, et al. Oh Passive (Amyloid- β) Immunotherapy attenuates monoaminergic axonal degeneration in the A β PPswe/PS1E9 mice. *J Alzheimer's Dis*. 2011;23:271–79. <https://doi.org/10.3233/JAD-2010-101602>.
67. Zhang Q, Yang C, Liu T, Liu L, Li F, Cai Y, et al. Citalopram restores short-term memory deficit and non-cognitive behaviors in APP/PS1 mice while halting the advance of Alzheimer's disease-like pathology. *Neuropharmacology*. 2018;131:475–86. <https://doi.org/10.1016/j.neuropharm.2017.12.021>. Published online
68. Nelson RL, Guo Z, Halagappa VM, Pearson M, Gray AJ, Matsuoka Y, et al. Prophylactic treatment with paroxetine ameliorates behavioral deficits and retards the development of amyloid and tau pathologies in 3xTgAD mice. *Exp Neurol*. 2007;205:166–76.
69. Cirrito JR, Wallace CE, Yan P, Davis TA, Gardiner WD, Doherty BM, et al. Effect of escitalopram on A β levels and plaque load in an Alzheimer mouse model. *Neurology*. 2020;95:2666. <https://doi.org/10.1212/WNL.0000000000010733>. Published online
70. Sheline YI, Snider BJ, Beer JC, Seok D, Fagan AM, Suckow RF, et al. Effect of escitalopram dose and treatment duration on CSF A β levels in healthy older adults: a controlled clinical trial. *Neurology*. 2020;95:2658 <https://doi.org/10.1212/WNL.0000000000010725>. Published online
71. Robert SJ, Lezoualc'h F. Distinct functional effects of human 5-HT $_4$ receptor isoforms on β -amyloid secretion. *Neurodegenerative Dis*. 2008;5:163–65. <https://doi.org/10.1159/000113691>.
72. Geldenhuys WJ, Van Der Schyf CJ. The serotonin 5-HT $_6$ receptor: a viable drug target for treating cognitive deficits in Alzheimer's disease. *Expert Rev Neurother*. 2009;9:1073–85. <https://doi.org/10.1586/ern.09.51>. Published online
73. Mattson MP, Maudsley S, Martin B. BDNF and 5-HT: a dynamic duo in age-related neuronal plasticity and neurodegenerative disorders. *Trends Neurosci*. 2004;27:589–94. <https://doi.org/10.1016/j.tins.2004.08.001>. Published online

ACKNOWLEDGEMENTS

We gratefully acknowledge Karen Edmonds, Bineyam Gebrewold, Michael Hans, Jose Leon and David J. Clough for their invaluable contribution to the acquisition of PET data and to Terri Brawner, Ivana Kusevic and Kathy Kahl for their invaluable contribution to the acquisition of MRI data.

FUNDING

This study was supported by: National Institute of Health: MH064823 (GSS), MH086881 (GSS), AG038893 (GSS), AG041633 (GSS), AG059390 (GSS), UL1 TR 001079 (DEF), P30 AG019610 (Arizona Alzheimer's Disease Research Center [EMR]), the National Institute on Aging (EMR) and the state of Arizona (EMR).

COMPETING INTERESTS

The authors declare no competing interests.

ADDITIONAL INFORMATION

Correspondence and requests for materials should be addressed to Gwenn S. Smith.

Reprints and permission information is available at <http://www.nature.com/reprints>

Publisher's note Springer Nature remains neutral with regard to jurisdictional claims in published maps and institutional affiliations.



Open Access This article is licensed under a Creative Commons Attribution 4.0 International License, which permits use, sharing, adaptation, distribution and reproduction in any medium or format, as long as you give appropriate credit to the original author(s) and the source, provide a link to the Creative Commons license, and indicate if changes were made. The images or other third party material in this article are included in the article's Creative Commons license, unless indicated otherwise in a credit line to the material. If material is not included in the article's Creative Commons license and your intended use is not permitted by statutory regulation or exceeds the permitted use, you will need to obtain permission directly from the copyright holder. To view a copy of this license, visit <http://creativecommons.org/licenses/by/4.0/>.